HHS Public Access

Author manuscript

Wound Repair Regen. Author manuscript; available in PMC 2020 March 01.

Published in final edited form as:

Wound Repair Regen. 2019 March ; 27(2): 150–161. doi:10.1111/wrr.12692.

Discordance between histologic and visual assessment of tissue viability in excised burn wound tissue

Aos S. Karim, MD[1], **Amy Yan, BS**[1], **Edgar Ocotl, BS**[1], **Daniel D. Bennett, MD**[2], **Ziyue Wang, BS**[3], **Christina Kendziorski, PhD**[4], and **Angela L.F. Gibson, MD, PhD**[1]

[1]Department of Surgery, University of Wisconsin School of Medicine and Public Health

[2]Department of Dermatology, University of Wisconsin School of Medicine and Public Health

[3]Department of Statistics, University of Wisconsin

[4]Depertment of Biostatistics and Medical Informatics, University of Wisconsin

Abstract

The regenerative capacity of burn wounds, and the need for surgical intervention, depend on wound depth. Clinical visual assessment is considered the gold standard for burn depth assessment, but it remains a subjective and inaccurate method for tissue evaluation. The purpose of this study was to compare visual assessment with microscopic and molecular techniques for human burn depth determination, and illustrate differences in the evaluation of tissue for potential regenerative capacity. Using intraoperative visual assessment, patients were identified as having deep partial thickness or full thickness burn wounds. Tangential excisions of burn tissue were processed with hematoxylin and eosin to visualize tissue morphology, lactate dehydrogenase assay to ascertain cellular viability, and Keratin-15 and Ki67 to identify epidermal progenitor cells and proliferative capacity, respectively. RNA from deep partial and full thickness burn tissue as well as normal tissue controls were submitted for RNA sequencing. Lactate dehydrogenase, Keratin-15, and Ki67 were found throughout the excised burn wound tissue in both deep partial thickness burn tissues and in the second tangential excision of full thickness burn tissues. RNA sequencing demonstrated regenerative capacity in both deep partial and full thickness burn tissue, however a greater capacity for regeneration was present in deep partial thickness compared with full thickness burn tissues. In this study we highlight the discordance that exists between the intraoperative clinical identification of burn injury depth, and microscopic and molecular determination of viability and regenerative capacity. Current methods utilizing visual assessment for depth of injury are imprecise, and can lead to removal of viable tissue. Additionally, hematoxylin and eosin microscopic analysis should not be used as the sole method in research or clinical determination of depth, as there are no differences in staining between viable and nonviable tissue.

Corresponding author (and requests for reprints): Angela L.F. Gibson, MD, PhD, G5/339 CSC, 600 Highland Avenue, Madison, WI 53792-3236, Gibson@surgery.wisc.edu.

Financial Disclosure Statement: The authors have the following to disclose: None.

Keywords

Cellular viability; thermal injury; burn depth

Introduction

Skin has a remarkable ability to regenerate and repair itself. In deep burn wounds, the affected skin cells undergo necrosis and slough off, yet skin can still regenerate spontaneously if enough epithelial progenitor cells are present in the basal layer of skin appendages.[1] Based on an estimate of tissue viability and visual inspection of the wound bed, a surgeon decides whether to excise the wounded tissue or allow the skin to heal on its own. In essence, the surgeon determines the need for intervention in a burn injury by evaluating the depth of the burn.

Ever since the concept was first popularized by Dr. Zora Janzekovic in the 1970s, clinical visual assessment has been used to determine the depth of injury, as well as the adequacy of an excision.[1] In the United States, 80% of burn surgeons determine burn wound depth using visual assessment alone.[2] After visual assessment, Laser Doppler imaging is the most common technology used today.[3] The wound healing community continues to conduct research in the area of burn depth determination[4,5] and to develop new technologies for improving precision, both preoperatively and intraoperatively. The benefits and limitations of each technique are summarized in Table 1. However, the correlation between a visual diagnosis performed intraoperatively, and the microscopic assessment of wound viability and regenerative capacity, remains unknown.

While the majority of literature on wound healing and epithelialization describes experiments with animal models, most notably mice, mouse and human gene expression during inflammation are poorly correlated, and some doubt remains whether it is appropriate to translate the findings of mouse research to human disease.[6] Additionally, there are vast differences in wound healing between mice and humans (contraction of tissue in mice versus re-epithelialization in human skin), as well as in hair follicle density and location of sweat glands, further complicating the translation of animal studies.[7,8] The important contribution of sweat glands to re-epithelialization of wounds in humans was highlighted in a study demonstrating that sweat glands, which are present in skin at a density that is almost three-fold the density of hair follicles, extensively contribute to wound re-epithelialization.[9] This finding further emphasizes the concerns regarding the translation of prior research conducted in animals whose eccrine glands are absent, or significantly limited in presence.

The potential regenerative capacity in burn wounds has been suggested by studies investigating the use of excised burn eschar as a source of stem cells for wound repair.[10,11] By harnessing this regenerative capacity, we may be able to reduce the need for donor sites in deep partial thickness (DPT) burns. We hypothesized that DPT and full thickness (FT) burn wounds retain considerable viability and regenerative capacity that is not clinically apparent on visual inspection. Our study sought to characterize the baseline regenerative capacity in human burn wounds in correlation with their clinical visual depth diagnosis in order to understand the wound healing potential of DPT and FT depth burns.

Materials and methods

Patient identification and collection of intraoperative tissue and video images:

Patients with burn wounds were clinically assessed preoperatively by the operating surgeon, and were invited to participate in the study if their wounds required surgery. The decision to operate was based on stalled healing in DPT and indeterminate depth burns after a period of assessment of the trajectory of healing (7–14 days). Timing for surgery of FT burns was dependent on the healing of other areas of DPT burns in the same patient to reduce the overall amount of wound excised; in some cases the DPT wound was also grafted. Informed consent was obtained to collect human burn tissue excised during the surgical procedure prior to skin grafting. From the time of admission, all patients had their wounds washed with soap and water daily with bedside mechanical debridement by burn nurses. Bacitracin ointment and petroleum-impregnated gauze dressings were changed twice daily. Some of the FT burns were switched throughout their hospital course to silver sulfadiazine due to concern for bacterial overgrowth. This study was approved by the University of Wisconsin Human Subjects Committee Institutional Review Board in compliance with the 1975 Declaration of Helsinki. Intraoperatively, burn wound depth was determined by the burn surgeon using visual assessment prior to and during excision. Extremity burns were excised under tourniquet after Esmarch bandage exsanguination, and torso burns were excised after infiltration with epinephrine tumescence. Visual characteristics of the wound bed signaled the completion of excision, including pearly-appearing dermis, punctate bleeding, absence of thrombosed vessels, and/or glistening yellow fat. A digital video recording device was worn by the operating surgeon to record the intraoperative decision making process during tangential excision to enhance data collection for subsequent review. Intraoperative video footage was analyzed, and still image clips were identified that corresponded best to the time point in which a decision was made to continue or complete an excision. Five wounds clinically assessed as DPT burns and five wounds identified as FT burns were biopsied using a 4-mm sterile biopsy punch (Integra, York, PA) (Figure 1A). The area of the wound surrounding the biopsy punch was then removed in a sequential manner by tangential excision using a Goulian knife with a Weck blade, at a depth of approximately 400–500 microns thick to encompass the area of the biopsy (Figure 1B-C). Tissues were maintained in the correct anatomic alignment (noting superficial and deep surfaces) and order of excision (Figure 1D, 1–3). Normal skin tissue was also collected from reconstructive plastic surgery procedures as control skin.

Tissue processing:

Control and burn tissues were stored for up to one hour in normal saline prior to further processing. After bisecting the biopsies, one half was fixed in 1% PFA, 10% neutral buffered formalin (NBF) prior to paraffin embedding. The other half of the tissues were washed with Phosphate Buffered Saline (PBS) and fixed in 1% paraformaldehyde (PFA) for two hours on a shaker at 4°C, followed by overnight incubation in a 20% sucrose solution at 4°C. The following day, the fixed and sucrose-treated tissues were oriented in Tissue Tek OCT Compound (Fischer, Hampton, NH), frozen using liquid nitrogen, and prepared as ten-micron thick cryostat sections.

Histology and immunohistochemistry:

Five-micron thick paraffin embedded sections of burn tissue and normal controls were stained with hematoxylin and eosin (H&E). Cryostat sections were used for Keratin-15 (K15), Ki67 and lactate dehydrogenase (LDH) staining as previously described.[12,13]

LDH staining: Frozen sections were left out to air dry for a minimum of 2 hours (range 2–18 hours), then washed twice with PBS for 5 minutes each time. Sections were incubated with freshly prepared LDH solution containing 5% Polypep (Sigma, St. Louis, MO); 2mM Gly-Gly (Sigma, St. Louis, MO); 0.75% NaCl (Fisher, Hampton, NH); 60mM lactic acid (Dot Scientific Inc., Burton, MI); 1.75 mg/mL ß-nicotinamide adenine (Sigma, St. Louis, MO); and 3 mg/ml Nitroblue Tetrazolium (Sigma, St. Louis, MO) pH 8.0, for 3.5 hours at 37°C. Slides were washed twice for 2 minutes each with 50°C tap water, followed by two washes with PBS of 2 minutes each. Tissues were counterstained with aqueous eosin (Newcomer Supply, Middleton, WI) for 4 minutes. Slides were washed with PBS for 1 second, dehydrated with acetone for 30 seconds followed by acetone: xylene (1:1) for 1 minute, and finally with xylene alone for 1 minute. Slides were then cover slipped with Permount (Vector Laboratories, Burlingame, CA).

K15 staining: Indirect immunofluorescence (IIF) was used for K15. Sections were washed twice with PBS, blocked with 5% goat serum in PBS for one hour at room temperature, and then incubated with Anti-cytokeratin 15 antibody (1:200) (ab52816, Abcam, Cambridge, MA) overnight at 4°C. The tissues were incubated with Goat anti-rabbit IgG H&L Alexa-Fluor 568 (ab175471, Abcam, Cambridge, MA) for one hour at room temperature. The sections were then washed with PBS and the nuclei were counterstained with DAPI.

Ki67 staining: Cryostat sections were first acclimated to room temperature and then fixed with acetone for ten minutes. Afterwards, the sections were blocked with 2.5% normal horse serum (MP-7401, Vector Laboratories, Burlingame, Ca) for one hour at room temperature. Subsequently, the tissue sections were incubated with Anti-Ki67 antibody (1:500 dilution, ab16667, Clone number: SP6, Abcam, Cambridge, MA) diluted in 1% bovine serum albumin-PBS solution overnight at 4°C. On the following day, sections were incubated in 3% hydrogen peroxide-PBS solution for ten minutes to block endogenous peroxidase activity. The secondary antibody was then applied (MP-7401, Vector Laboratories, Burlingame, Ca) for 35 minutes. After incubation with the secondary antibody, sections were visualized by incubating with 3,3′-diaminobenzidine solution (Vector Laboratories, Burlingame, Ca) for two minutes. Tris-Buffered Saline containing Tween 20 was used for rinsing the sections in between steps. Tissue sections were then counterstained with hematoxylin, dehydrated using a graded alcohol series (95, 100), and cleared with xylene. Finally, sections were mounted with Richard-Allan Mounting Medium (VWR, Radnor, PA).

Image capture analysis: Tissue sections were viewed using a Nikon Ti-S inverted microscope and digital images were captured with Nikon DS Ri2 cooled color camera, X-Cite 120LED BOOST System lamp from Excelitas, and Nikon Imaging Software, NIS Elements (Nikon, Tokyo, Japan). Bright field images of H&E, LDH, and Ki67 were taken at

40X magnification. IIF images were captured at 40X for K15 and using filters for Texas Red (K15) and DAPI (nuclear) and the images were then merged using NIS elements software.

Pathology review:

A board-certified dermatopathologist blinded to the burn depth determination of each sample performed histopathological evaluation on all H&E stained sections using characteristics of the tissue including the epithelial lining of the skin appendages (hair follicles and eccrine ducts/glands), blood vessels, fat, smooth muscle, collagen appearance, cellular infiltrate, and presence of epithelialization. Representative samples were chosen for figures in the manuscript.

RNA sequencing:

Samples clinically estimated to be DPT or FT (Figure 2) were sent for RNA isolation and sequencing along with normal controls (NL) obtained from skin discarded in reconstructive operations. Tissue samples were flash frozen and stored at −80°C prior to submission to the Biotechnology Center at the University of Wisconsin for mRNA extraction and sequencing. RNA was extracted using Illumina TruSeq Stranded Total RNA Library Prep Kit (Cat. # 20020594, Ilumina, San Diego, CA), quality control of the samples was done on Agilent DNA1000 (Agilent Technologies, Santa Clara, CA) and sequencing done on Ilumina HiSeq 2000.

Statistical Analysis:

Reads were mapped back to the genome using the short read aligner Bowtie[14] followed by RSEM[15] to estimate gene expression. EBSeq[16] was applied to identify differentially expressed genes (DEG). Null hypotheses tested in EBSeq were FT=NL, DPT=NL and FT=DPT. DEGs were defined as those having posterior probability of DEG greater than 0.95 as this controls the expected false discovery rate at 5%.[16] Gene Enrichment analysis was done using the Gene Set Enrichment Analysis (GSEA) software.[17] Heat maps were created with Morpheus.[18]

A literature and Gene Ontology search identified 245 genes associated with inflammatory response and 249 genes involved in regenerative capacity of epithelium that were DE in both the DPT versus Normal and FT versus Normal tissue. In addition, these genes had fold changes (FC) of DPT to Normal [FC(DPT:NL)] and FT to Normal [FC(FT:NL)] larger than 1.5 or smaller than −1.5. A one-sided, paired T-test was applied to $\log_2$-transformed fold changes to test the null hypothesis H0:FC(DPT:NL) > FC(FT:NL) or FC(DPT:NL) < FC(FT:NL) for these genes. Statistics and graphing were done in R.[19]

Results

Intraoperative Visual Assessment with Videography

Still frames from the videography of DPT and FT burn wounds demonstrate the changes in color and texture that occur with tourniquet application (Figure 3A1 to 3A2). Additionally, segments obtained from video footage of wounds not under tourniquet allowed assessment of the wound after a period of time (6 seconds) to illustrate adequate wound perfusion

(Figure 3B3 to 3B4). Characteristics that are historically used for visual assessment of depth of injury during tangential excision of burn wounds[1] are visible using the video images, including pearly dermis (arrow in Figure 3A3), absence of thrombosed vessels (presence of thrombosed vessels denoted by arrows in Figure 3B2), bright yellow fat (visible through the remaining reticular dermis by arrow in Figure 3B3), and punctate bleeding (arrows in Figure 3B4). Each of the five burn wounds identified prior to excision as DPT only required one tangential excision, however each of the five burn wounds identified as FT required at least two tangential excisions consistent with a deeper injury in the FT burn samples.

In order to validate our intraoperative assessment of the burn wounds, digital images of the burn wounds that were obtained prior to excision were sent in an anonymous electronic survey to thirty-five burn surgeons who were instructed to choose whether the circled area in the image represented a DPT or FT burn (Figure 2). Responses were correlated to our own assessments in the operating room. There was an 80–100% (average 90%) consensus between the burn surgeons with respect of visual estimation of the depth (Figure 2 insets).

Histologic Examination

We utilized two histologic staining methods, H&E and LDH, to assess the cellular viability of the tissue. We have previously shown that LDH staining is a simple method that more consistently measures cellular viability.[20] In some burns clinically identified as DPT, the LDH assay revealed viability of the majority of the tissue, as indicated by blue staining into the mid to upper portion of the first tangential excision (Figure 4B; preoperative image Figure 2G), equating the depth microscopically to a superficial partial thickness burn. In other burns identified clinically as DPT, a thin layer of epithelium was evident microscopically that appeared to have emanated from the hair follicle, consistent with re-epithelialization in the middle of the wound (Figure 5A; preoperative figure 3A2). The LDH assay on this DPT burn wound revealed viability of the whole tissue, as indicated by blue staining throughout (Figure 5B), and also demonstrated the immature layer of re-epithelialization.

Tissue in the first tangential excision layer of burns identified clinically as a FT wound (preoperative figure 1A), showed evidence of necrotic skin appendages on H&E staining, with the appearance of an abnormal but not necrotic inferior portion of the hair follicle (Figure 4C arrow). There was minimal staining of LDH in the superficial portions of the first tangential excision, which likely corresponds to fibroblasts and scattered inflammatory cells, confirming the lack of viability in this portion of the injured tissue (Figure 4D). However, as the wound was excised deeper, structures with viable appearance were more easily identified by LDH assay in the subsequent layer (Figure 4F).

Regenerative Capacity

To determine if cellular viability was associated with regenerative capacity of the excised tissue, we performed immunohistochemistry for K15, a basal keratinocyte marker located in the basal cell layer and hair bulge stem cells, and associated with progenitor epithelial cells, [21,22] as well as Ki67 nuclear staining to identify proliferating cells. In the normal unburned adult skin tissue, K15 is localized to the basal layer of keratinocytes in the interfollicular

epidermis, as well as the epithelial lining of the skin appendages (Figure 6C). K15 was present along the basal layer of re-epithelializing tissue and the skin appendages located deeper within the dermis in DPT burn tissue, however the K15 positive cells represent a subset of all cells that had normal tissue architecture on H&E or viability on LDH staining (Figure 6E-G). As expected, FT burn tissue lacked K15 staining in the superficial tissue, consistent with the lack of viability identified on H&E and LDH staining (Figure 6I-K). In the deeper regions of the FT burn tissue, K15 positive cells were located within the eccrine and hair follicle appendages (Figure 6K). This tissue was ultimately excised and discarded surgically due to the visual appearance of necrotic tissue, as demonstrated in Figure 1B.

Cellular proliferation, measured by Ki67 expression, was low in normal unwounded adult skin (Figure 6D arrows), as previously reported in the literature.[23] However, excised burn tissue from DPT burns exhibited increased expression throughout most skin appendages and re-epithelialized tissue (Figure 6H arrows). Ki67 positive cells were also present in the deeper region of FT burn tissue, corresponding to tissue that was assessed intraoperatively as necrotic and requiring excision (Figure 6L arrows).

RNA sequencing:

To determine if the histological markers of viability and regenerative capacity were also seen on the molecular level, full thickness tissue biopsies obtained intraoperatively and clinically assessed to be DPT or FT were submitted for RNA sequencing. There were 5416 differentially expressed genes (DEG) identified in FT and 4131 DEG in DPT tissues. 1442 of the DEG were different in DPT versus FT. The top 20 enriched pathways in DPT were related to regeneration while inflammation and oxidative stress pathways were significantly enriched in FT tissues (Supplemental Figure 1). A close examination of the regenerative genes in DPT and FT (Supplemental Table 1) shows that genes involved in the epidermal growth factor pathway such as EGFR, EGF, ERBB2, ERBB3, ERBB4, amongst other epithelial growth factors are overall downregulated in these tissues compared with the normal tissues. When comparing DPT and FT gene sets for inflammation and regeneration, DPT had greater regenerative potential than FT (Figure 7A; $p<0.03$), while FT had greater inflammatory response and reactive oxygen species (ROS) than DPT (Figure 7B; $p<0.0001$).

Discussion

Our results support the hypothesis that there is discordance between characteristics of the wound bed that are apparent on a macroscopic level using unaided visual assessment, and the viability and regenerative capacity of this tissue assessed on a microscopic and molecular level. This discordance was perhaps the most striking in wounds that were identified preoperatively as FT. However, these discrepancies were also evident with DPT wounds. For example, the level of re-epithelialization that was evident microscopically in wounds thought to be DPT was unexpected, although in hindsight, could be explained by the length of time the burn was allowed to heal prior to surgery (7–14 days for DPT samples). The surgeon's visual assessment at 10 days after injury in the representative sample, shown in the pre-excision video image clip in Figure 2A, failed to accurately capture the viability identified on the H&E and LDH stained sections of DPT burns. These findings correlated with RNA

sequencing data, which showed that regenerative genes were still expressed in the DPT tissues. This discordance resulted in the intraoperative decision to excise the perceived necrotic tissue and graft with autologous donor skin. Visual detection of the epithelialization was likely obscured by a thin layer of pseudoeschar that often accumulates on the surface of the wound from general fibrinous exudate produced in an open wound. Given the lack of a fully mature stratified tissue, the surface of the wound clinically appeared wet, signifying a lack of barrier function. The expression of K15 and Ki67 in the excised burn tissues that was evident in the deeper skin appendages (e.g. hair follicle and eccrine glands) suggests that this tissue is capable of autologous regeneration in a supportive wound healing environment. The delay in healing could be a result of the imbalance at the molecular level between inflammatory factors and epidermal regeneration factors as evident on the RNA sequencing data.

Our results also demonstrate that the naked eye is incapable of perceiving this regenerative capacity, despite the characteristics that we currently associate with viable tissue. These findings are noteworthy when it comes to comparing clinical outcomes. In clinical trials for burn treatments, surgeons often prepare the wound bed using visual evaluation only; if the wound bed preparations are not standardized across patients (e.g. excision leaving similar amounts of healthy dermis using the same characteristics), comparison of outcomes may be challenging or even misleading.

Further, the use of standard H&E staining methods alone to determine viability of tissue often makes it difficult to interpret current literature on wound healing. We have shown that LDH staining improves the ability to identify viable tissue,[20] and makes it easier to detect burn wound depth and to perform adequate excision in a pre-clinical research setting. However, this stain is impractical for intraoperative use due to the time required for tissue processing and staining. Our results suggest that, in addition to identification of the visual characteristics indicating adequate excision, there is a need for further evaluation of the wound bed in order to normalize the wound bed for comparison of outcomes, prior to application of new technologies such as biologic tissue substitutes. The results of these types of tissue substitutes often depend upon the quality of the wound bed on which they are placed. Non-invasive imaging technologies for estimation of burn wound healing[24,25] could be modified for intraoperative use after co-registration of wound bed features obtained with non-invasive imaging and microscopic characteristics such as those identified in this study.

Videography is useful for documentation of intraoperative decision-making and wound characteristics, to analyze later in a research setting, and can provide a library of examples for teaching residents and fellows of the art of burn surgery. Videography can be easily incorporated into practice in multiple ways. For example, it can be performed using a head-mounted video camera as in our study, with a camera mounted on a boom over the surgical field, or by using a smartphone camera, as was done in some of our samples. These newer, high-resolution video cameras provide an exceptional level of detail that can be captured even under operating room lighting.

Limitations

Limitations to this study include the small sample size and the single institution setting. The visual interpretation of burn wound depth is subjective, using learned visual cues to formulate the assessment. The simplified designation of our samples as DPT or FT categories, determined in the operating room immediately prior to excision, was purposeful to aid our data analyses. While only two surgeons were engaged to determine depth in this study, we did try to increase our confidence in our assessments through an informal survey to 35 burn surgeons using photographs of burns at the time of excision. The following language was used in the survey: “After reviewing this image, do you feel the area in the black circle is a full thickness injury (i.e. little to no dermis will be left after excision) or a deep partial thickness injury (excision will leave healthy dermis in the wound bed)”. The use of images in this manner is a very crude substitute for in person assessment, and some features such as pseudoeschar, vascularity and moisture in the wound are hard to assess. However, we found an average of 90% agreement with visual depth determination across all samples (Figure 2 insets). We recognize that the category of DPT is much more variable than FT and our data demonstrate that the vast amount of FT burns are actually DPT, however the true regenerative potential of DPT wounds is not well described in any studies to date. Finally, we only investigated epithelial cell markers for our study, however other sources for epithelialization are also recognized such as adipose, mesenchymal and bone marrow derived stem cells.[11]

Conclusions

Our findings advance the idea of harnessing the potential autologous regenerative capacity within the burn wound. For example, a recent study using laser Doppler imaging to classify indeterminate depth burns into high, intermediate, and low healing potential concluded that there was no benefit on scar quality or healing time with surgical treatment of wounds classified as having intermediate healing potential.[26] Therefore, opportunities exist for wound healing to occur without the need for a donor site in wounds previously treated with an “early excision and grafting” philosophy.[27] This shift to a wait-and-see approach could utilize technologies developed to detect the regenerative capacity of each wound, and tailor treatment accordingly. However, an improved understanding of the specific wound bed characteristics, and the treatment needed to harness the inherent regenerative capacity in these wounds, will be required before a paradigm shift can occur.

Supplementary Material

Refer to Web version on PubMed Central for supplementary material.

Acknowledgements:

Support for the RNA sequencing in the project is provided by the UW SDRC grant P30 AR066524, funded by the National Institute of Arthritis, Musculoskeletal and Skin disease (NIAMS).

External Funding:

University of Wisconsin Skin Disease Research Center grant P30 AR066524, funded by the National Institute of Arthritis, Musculoskeletal and Skin disease (NIAMS).

List of Abbreviations:

DEG	Differentially Expressed Genes
DPT	Deep Partial Thickness
EGF	Epidermal Growth factor
EGFR	Epidermal Growth Factor Receptor
ERBB	erbB Tyrosine Receptor Kinase
FC	Fold Change
FT	Full Thickness
GSEA	Gene Set Enrichment Analysis
H&E	Hematoxylin and Eosin
K15	Keratin 15
LDH	Lactate Dehydrogenase
NBF	Natural Buffered Saline
NL	Normal Tissue
PBS	Phosphate Buffered Saline
PFA	Paraformaldehyde
RNA	Ribonucleic Acid
ROS	Reactive Oxygen Species
TE	Tangential Excision

References:

1. Janzekovic Z A New Concept in the Early Excision and Immediate Grafting of Burns. Journal of Trauma 1970;10(12):1103–1108. [PubMed: 4921723]
2. Israel JS, Greenhalgh DG, Gibson AL. Variations in Burn Excision and Grafting: A Survey of the American Burn Association. J Burn Care Res 2017;38(1):e125–e132. [PubMed: 27893575]
3. Khatib M, Jabir S, Fitzgerald O'Connor E, Philp B. A systematic review of the evolution of laser Doppler techniques in burn depth assessment. Plast Surg Int 2014;2014:621792. [PubMed: 25180087]
4. Jaskille AD, Shupp JW, Jordan MH, Jeng JC. Critical review of burn depth assessment techniques: Part I. Historical review. J Burn Care Res 2009;30(6):937–947. [PubMed: 19898102]
5. Jaskille AD, Ramella-Roman JC, Shupp JW, Jordan MH, Jeng JC. Critical review of burn depth assessment techniques: part II. Review of laser doppler technology. J Burn Care Res 2010;31(1): 151–157. [PubMed: 20061851]
6. Seok J, Warren HS, Cuenca AG, et al. Genomic responses in mouse models poorly mimic human inflammatory diseases. Proc Natl Acad Sci U S A 2013;110(9):3507–3512. [PubMed: 23401516]

7. Boyko TV, Longaker MT, Yang GP. Laboratory Models for the Study of Normal and Pathologic Wound Healing. Plast Reconstr Surg 2017;139(3):654–662. [PubMed: 28234843]
8. Pastar I, Wong LL, Egger AN, Tomic-Canic M. Descriptive vs mechanistic scientific approach to study wound healing and its inhibition: Is there a value of translational research involving human subjects? Exp Dermatol 2018;27(5):551–562. [PubMed: 29660181]
9. Rittié L, Sachs DL, Orringer JS, Voorhees JJ, Fisher GJ. Eccrine sweat glands are major contributors to reepithelialization of human wounds. Am J Pathol 2013;182(1):163–171. [PubMed: 23159944]
10. Natesan S, Wrice NL, Baer DG, Christy RJ. Debrided skin as a source of autologous stem cells for wound repair. Stem Cells 2011;29(8):1219–1230. [PubMed: 21674701]
11. van der Veen VC, Vlig M, van Milligen FJ, de Vries SI, Middelkoop E, Ulrich MM. Stem cells in burn eschar. Cell Transplant 2012;21(5):933–942. [PubMed: 21944933]
12. Gibson AL, Shalini Shatadal. A simple and improved method to determine cell viability in burn-injured tissue. Journal of Surgical Research 2017;215:83–87. [PubMed: 28688666]
13. Stoddart MJ, Furlong PI, Simpson A, Davies CM, Richards RG. A comparison of non-radioactive methods for assessing viability in ex vivo cultured cancellous bone: technical note. Eur Cell Mater 2006;12:16–25; discussion 16–25. [PubMed: 16888702]
14. Langmead B, Trapnell C, Pop M, Salzberg SL. Ultrafast and memory-efficient alignment of short DNA sequences to the human genome. Genome Biol 2009;10(3):R25. [PubMed: 19261174]
15. Li B, Dewey CN. RSEM: accurate transcript quantification from RNA-Seq data with or without a reference genome. BMC Bioinformatics 2011;12:323. [PubMed: 21816040]
16. Leng N, Dawson JA, Thomson JA, et al. EBSeq: an empirical Bayes hierarchical model for inference in RNA-seq experiments. Bioinformatics 2013;29(8):1035–1043. [PubMed: 23428641]
17. Gene set enrichment analysis: A knowledge-based approach for interpreting genome-wide expression profiles [computer program] Version 3.0: PNAS; 2005.
18. Morpheus: Versatile matrix visualization and analysis software [computer program] Broad Institite; 2018.
19. R: A language and environment for statistical computing [computer program] R Foundation for Statistical Computing; 2018.
20. Gibson ALF, Bennett DD, Taylor LJ. Improving the histologic characterization of burn depth. J Cutan Pathol 2017;44(12):998–1004. [PubMed: 28632906]
21. Guo A, Jahoda CA. An improved method of human keratinocyte culture from skin explants: cell expansion is linked to markers of activated progenitor cells. Exp Dermatol 2009;18(8):720–726. [PubMed: 19558495]
22. Ito M, Liu Y, Yang Z, et al. Stem cells in the hair follicle bulge contribute to wound repair but not to homeostasis of the epidermis. Nat Med 2005;11(12):1351–1354. [PubMed: 16288281]
23. Patel GK, Wilson CH, Harding KG, Finlay AY, Bowden PE. Numerous keratinocyte subtypes involved in wound re-epithelialization. J Invest Dermatol 2006;126(2):497–502. [PubMed: 16374449]
24. Paul DW, Ghassemi P, Ramella-Roman JC, et al. Noninvasive imaging technologies for cutaneous wound assessment: A review. Wound Repair Regen 2015;23(2):149–162. [PubMed: 25832563]
25. Sen CK, Ghatak S, Gnyawali SC, Roy S, Gordillo GM. Cutaneous Imaging Technologies in Acute Burn and Chronic Wound Care. Plast Reconstr Surg 2016;138(3 Suppl):119S–128S. [PubMed: 27556752]
26. Goei H, van der Vlies CH, Hop MJ, et al. Long-term scar quality in burns with three distinct healing potentials: A multicenter prospective cohort study. Wound Repair Regen 2016;24(4):721–730. [PubMed: 27102976]
27. Merz KM, Pfau M, Blumenstock G, Tenenhaus M, Schaller HE, Rennekampff HO. Cutaneous microcirculatory assessment of the burn wound is associated with depth of injury and predicts healing time. Burns 2010;36(4):477–482. [PubMed: 19854578]
28. Sharma VP, O'Boyle CP, Jeffery SL. Man or machine? The clinimetric properties of laser Doppler imaging in burn depth assessment. J Burn Care Res 2011;32(1):143–149. [PubMed: 21107272]

29. Hop MJ, Stekelenburg CM, Hiddingh J, et al. Cost-Effectiveness of Laser Doppler Imaging in Burn Care in The Netherlands: A Randomized Controlled Trial. Plast Reconstr Surg 2016;137(1):166e–176e.

30. Jeng JC, Bridgeman A, Shivnan L, et al. Laser Doppler imaging determines need for excision and grafting in advance of clinical judgment: a prospective blinded trial. Burns 2003;29(7):665–670. [PubMed: 14556723]

31. Thatcher JE, Li W, Rodriguez-Vaqueiro Y, et al. Multispectral and Photoplethysmography Optical Imaging Techniques Identify Important Tissue Characteristics in an Animal Model of Tangential Burn Excision. J Burn Care Res 2016;37(1):38–52. [PubMed: 26594863]

32. Prindeze NJ, Fathi P, Mino MJ, et al. Examination of the Early Diagnostic Applicability of Active Dynamic Thermography for Burn Wound Depth Assessment and Concept Analysis. J Burn Care Res 2015;36(6):626–635. [PubMed: 25412050]

33. Altintas MA, Altintas AA, Knobloch K, Guggenheim M, Zweifel CJ, Vogt PM. Differentiation of superficial-partial vs. deep-partial thickness burn injuries in vivo by confocal-laser-scanning microscopy. Burns 2009;35(1):80–86. [PubMed: 18691820]

34. Kaiser M, Yafi A, Cinat M, Choi B, Durkin AJ. Noninvasive assessment of burn wound severity using optical technology: a review of current and future modalities. Burns 2011;37(3):377–386. [PubMed: 21185123]

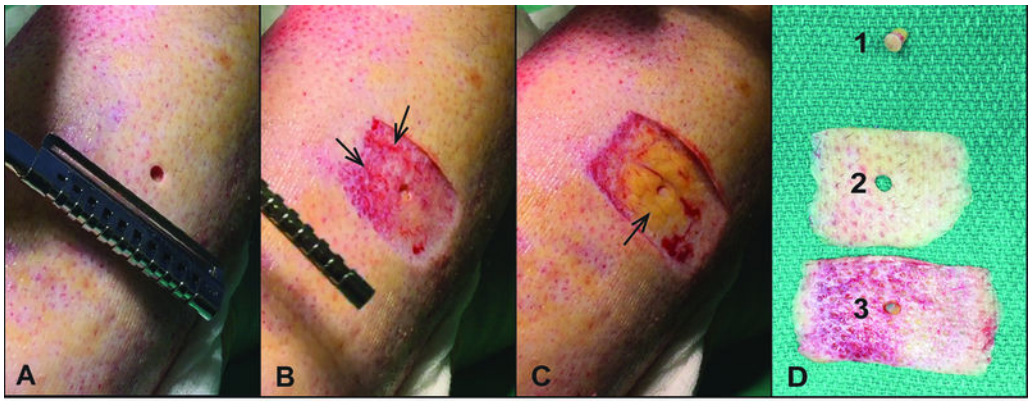

Figure 1 –. Intraoperative videography illustrates surgical decision making for excision of burn injured tissue.

Representative patient samples of intraoperative video clips (A-C) of tangential excision (TE) under tourniquet of burned extremity. Biopsy and sequential tangential samples of excised burn tissue were maintained in correct orientation and alignment to capture the superficial to deep excision (D). A) Pre-excision biopsy through burn wound clinically assessed as full thickness at the time of surgery. B) Wound bed after the first tangential excision. Note the hemorrhagic tissue with devitalized appearing dermis, which signified incomplete excision of burn wound (arrows). C) Wound bed after final tangential excision showing healthy appearing fat (arrow). D) Tissue samples corresponding to biopsy (1), first tangential excision (2), and final excision (3).

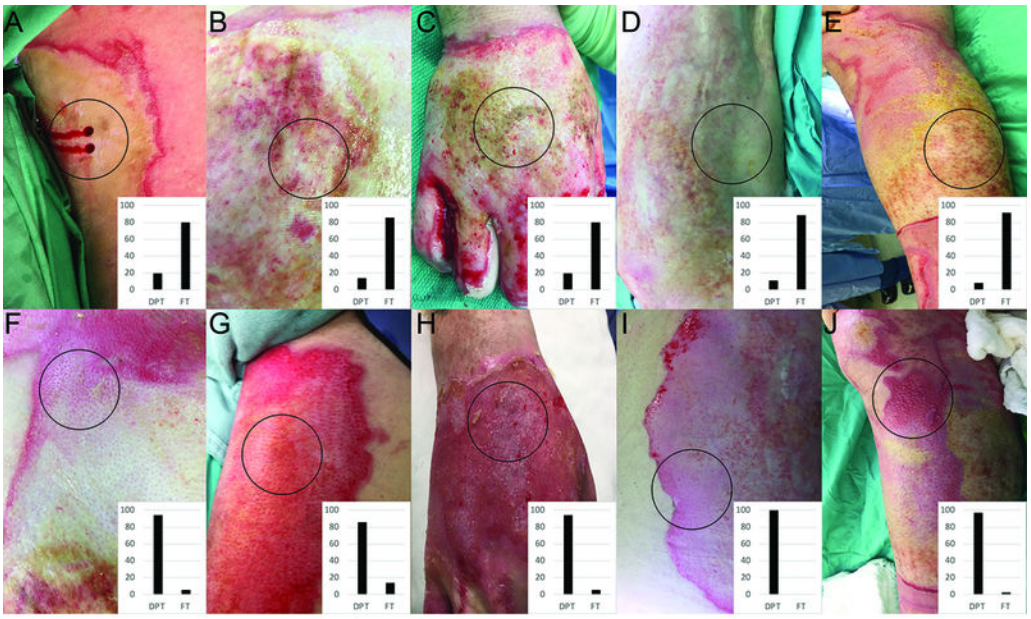

Figure 2 –. Intraoperative images of patients with deep partial and full thickness burns prior to excision.

Still frames from intraoperative videos of five patients with DPT and five patients with FT burns. Insets show percentage of surgeons choosing DPT or FT depth of burn based on visual evaluation. Circles denoted the area that the surgeons were asked to evaluate.

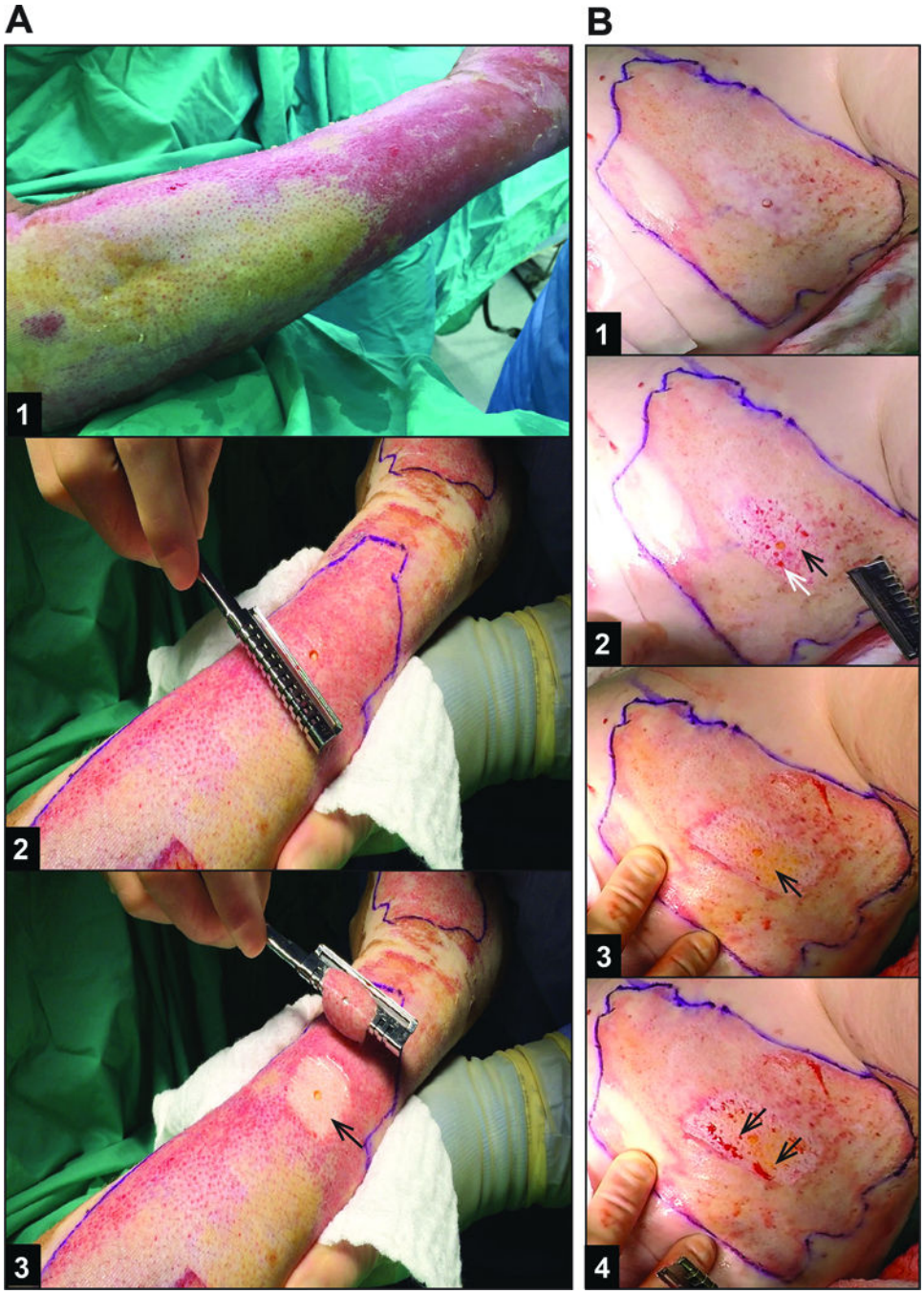

Figure 3 –. Methods of hemostasis during excision influence visual assessment of tissue viability.
Representative patient samples of still frames from (A) an area of DPT burn excision under tourniquet and (B) FT burn excision under epinephrine tumescence without tourniquet. A1) DPT burn 10 days after injury, prior to tourniquet placement – note the heterogeneity of the burn wound with more healing having occurred in wound on the right side of the image. A2) DPT burn with biopsy after tourniquet inflated prior to excision. A3) Wound bed after 1st and only TE required to reach healthy appearing dermis (arrow). B1) FT burn 7 days after injury, after infiltration with epinephrine tumescence (flank burn). B2) Wound bed after 1st

TE. Arrows indicate non-viable appearing dermis with thrombosed vessels (black arrow) and intermixed punctate bleeding (white arrow), indicating the need for further excision. B3) Wound bed after 2nd and final TE with arrow indicating healthy appearing dermis, fat, and absence of thrombosed vessels. B4) Same wound bed as in B3 after 6 seconds, showing punctate bleeding (arrows), and confirming viable, perfused wound bed.

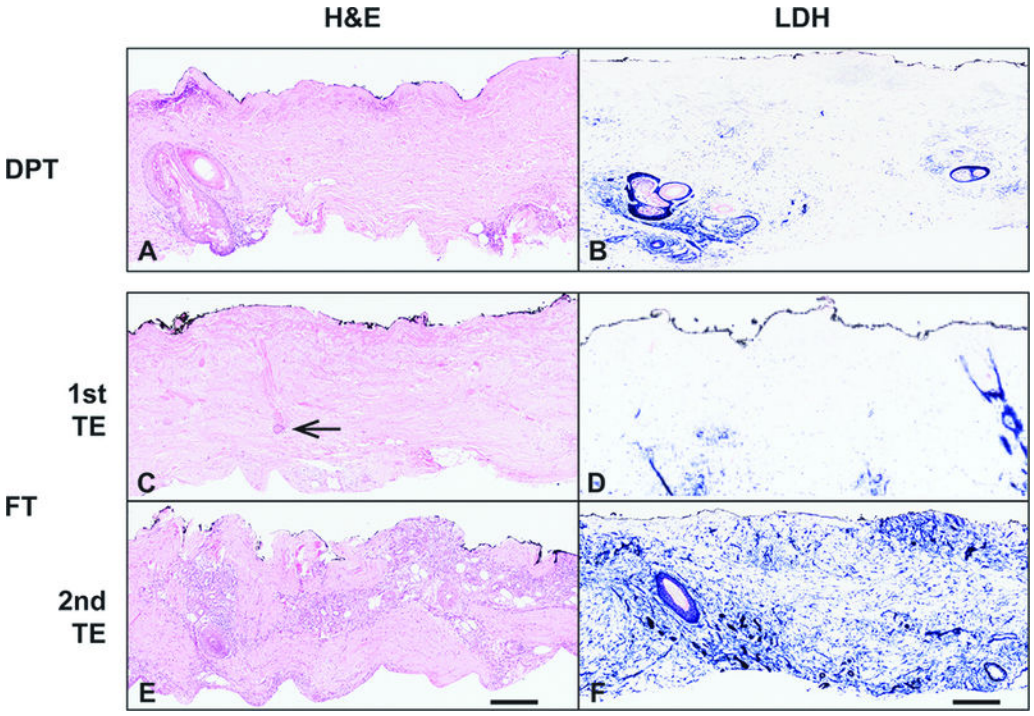

Figure 4 –. Viability staining reveals the level of tissue necrosis.

A) H&E staining of a DPT burn. B) LDH staining of same burn wound as in A. C). H&E stain of the 1st TE in FT tissue with necrosis of the upper portions of the excision. The inferior portion of a hair follicle retains aberrant but not clearly necrotic cells (arrow). The 2nd TE contains normal appearing cellularity and skin appendages throughout the tissue. LDH stain sections corresponding to the 1st and 2nd TE reveal viability partially through the 1st TE and throughout the entire 2nd TE. Scale bar = 300 microns. Representative patient samples were chosen.

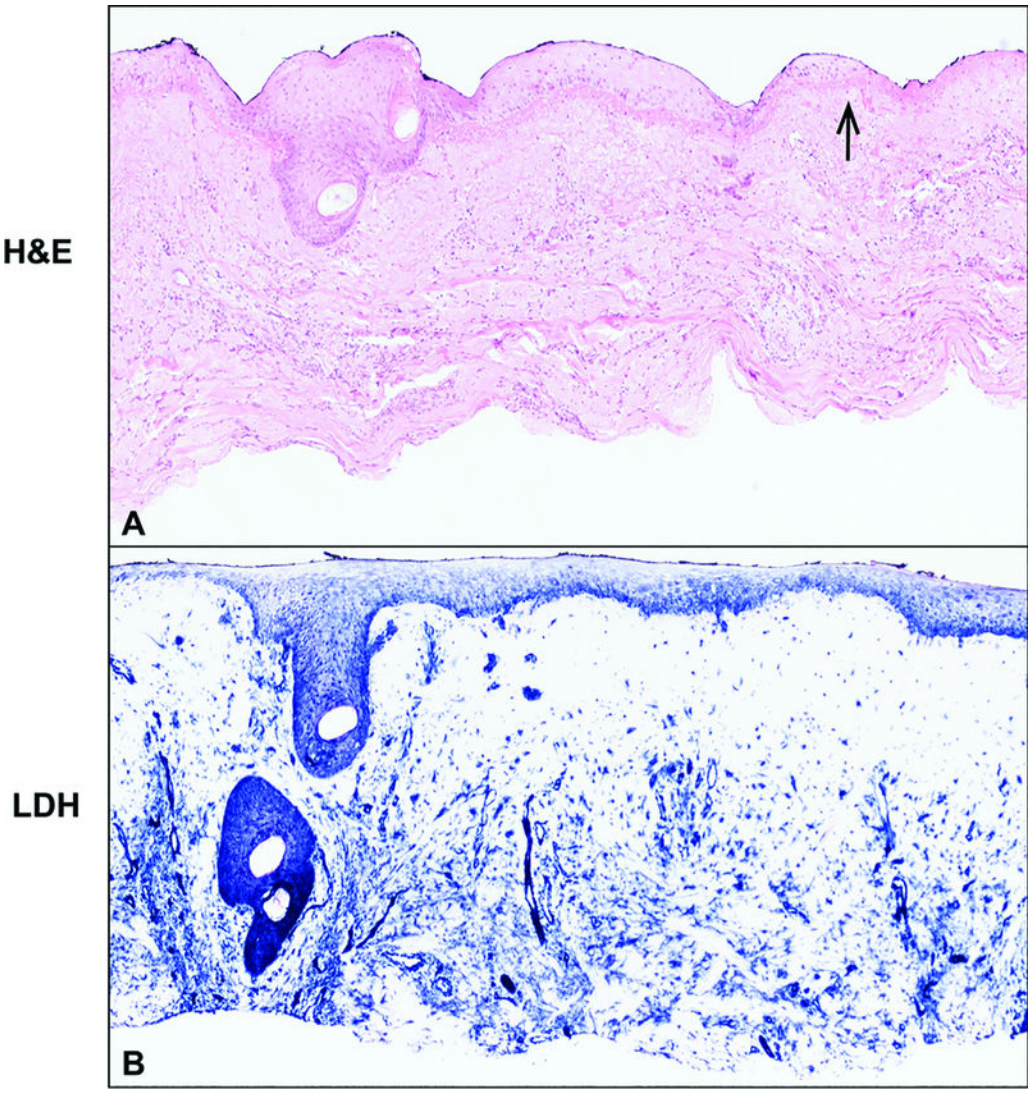

Figure 5 –. Clinically assessed DPT wound has microscopic evidence of re-epithelialization.
A) H&E stain of DPT TE demonstrating normal hair follicle and re-epithelialization from this structure. Arrow points to a thin layer of epithelium that appeared to have emanated from the hair follicle. B) Blue LDH stain confirming viability throughout the tissue.

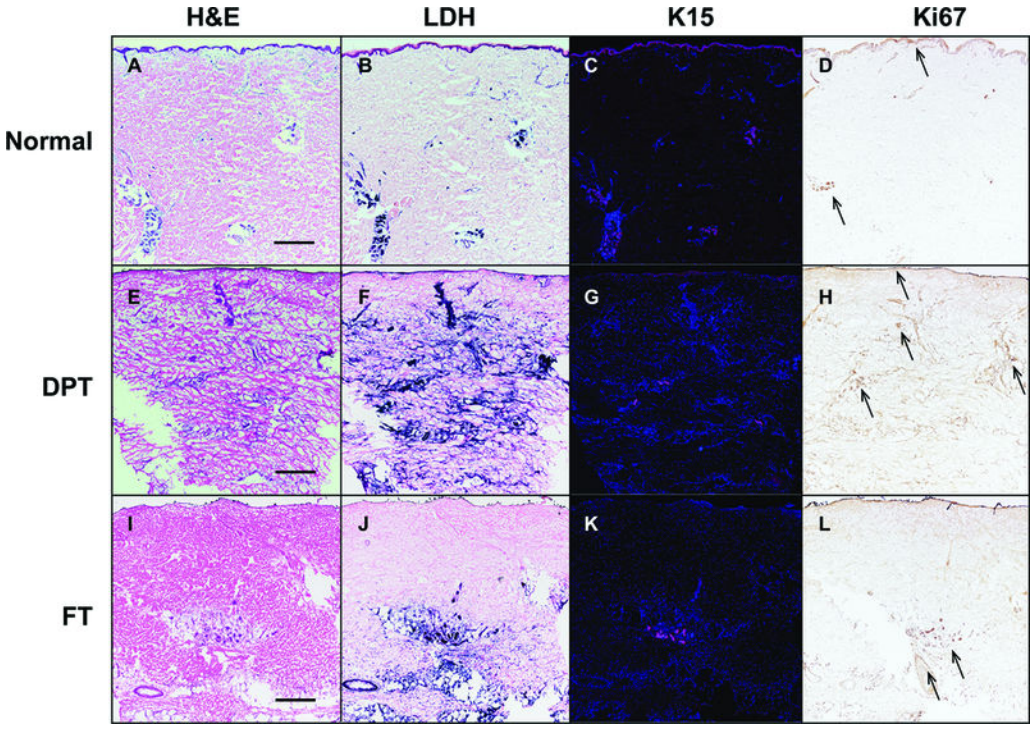

Figure 6 –. Epidermal progenitor cells are present in clinically diagnosed deep partial and full thickness burns.

Representative sections of normal (A-D), clinically determined DPT (E-H; corresponding clinical figure 3A2), and FT (I-L; corresponding clinical figure 1A) tissue sections stained for H&E, LDH (blue), K15 (magenta fluorescence), and Ki67 (brown nuclear) demonstrating the correlation between normal appearing cellular architecture (A, E, I), viable cells (B,F,J), expression of an epidermal progenitor marker K15 (C, G, K) and proliferation marker Ki67 (arrows in D, H, L). Scale bar = 200 microns. Representative patient samples were chosen.

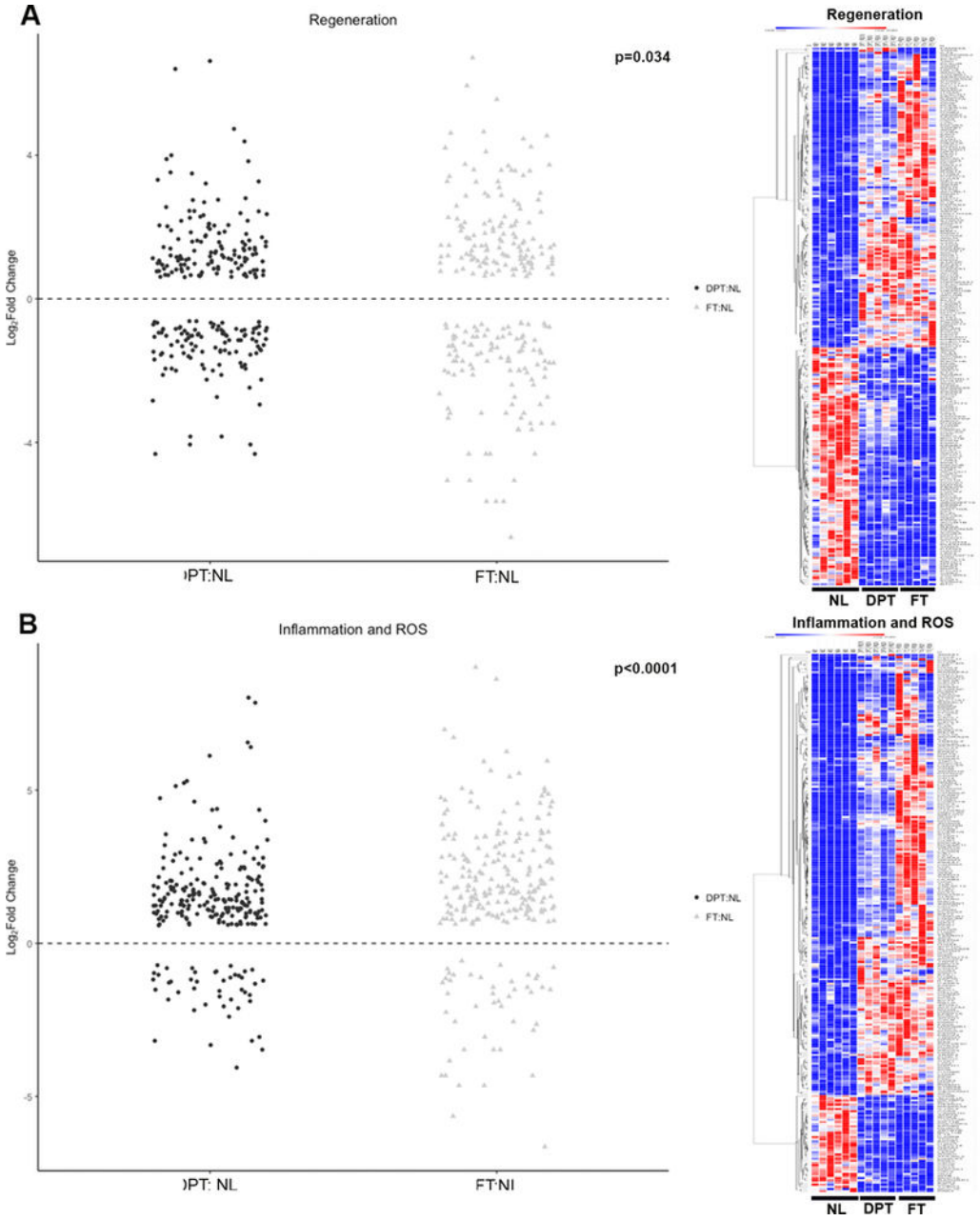

Figure 7 –. Analysis of gene sets of genes involved in inflammation of regeneration.

Legend: DPT: Deep partial thickness. FT: Full thickness. NL: Normal tissue. For Jitter plots, each gene is represented with a dot on the Y axis indicating its expression. For the heat maps, each column represents a sample (6 normal, 5 DPT burn and 5 FT burns), while each row represents a single gene. Red indicates greater expression relative to the mean expression of other samples in the same row. Blue indicates lower expression. A) Genes involved in regeneration. Jitter plot and heat map showing that while regenerative genes are overall downregulated relative to normal tissues, DPT had more regenerative capacity than FT tissues. B) Genes involved in inflammation. Jitter plot and heat maps showing that while

inflammatory genes are upregulated in both DPT and FT relative to normal tissues, FT had a greater inflammatory gene expression relative to DPT tissues.

Table 1 –

Summary of various burn depth detection methods

Methods of depth determination	Pro	Con
Currently available		
Clinical visual evaluation[1]	Inexpensive, readily available.	Subjective, requires experience.
Wound biopsy[4]	"Gold standard," extensive literature over many years.	Subjective, small sample size leads to errors due to heterogeneity of wounds.
Laser Doppler Imaging (LDI)[28–30]	Easy to use, non-contact, established protocols, currently in use worldwide.	Relies upon blood flow. Difficult to interpret with vasoconstriction injection or tourniquet use.
Under development		
Multispectral (MSI) and Photoplethysmography (PPG) Optical Imaging[31]	Can be used intraoperatively. Distinguishes viable from burn tissue using machine learning algorithms.	MSI can misclassify tissue leading to false interpretation. PPG relies upon blood flow. Difficult to interpret with vasoconstriction injection or tourniquet use.
Active Dynamic Thermography[32]	Non-contact, distinguishes tissue of different thermal conductivities.	Thermal differences in tissue are affected by ambient temperature.
In vivo confocal-laser-scanning microscopy[33]	Non-contact, detects changes on a histomorphometric level, currently used in dermatology.	Applicability to intraoperative use is unclear. Limited of detection at 350 μm – incomplete evaluation of deep partial thickness burn. Long imaging acquisition time (~10 minutes).
Indocyanine green videoangiography[34]	Rapid, compact device, currently used for microvascular flow in reconstructive surgery.	Interpretation in burn injury not well defined. Relies upon blood flow. Difficult to interpret with vasoconstriction injection or tourniquet use.
Near-infrared imaging spectroscopy[24]	Identifies skin chromophores including water content to distinguish between various burn depths, non-contact.	Not clinically validated.
Optical coherence tomography[31]	High resolution, multisectional. Can differentiate epidermis and dermis to evaluate epithelialization. Real-time imaging.	Limited depth penetration power. Expensive, small field of view, long imaging acquisition time (~5 minutes).